

LLaVA-MORE : A Comparative Study of LLMs and Visual Backbones for Enhanced Visual Instruction Tuning

Federico Cocchi^{1,2*} Nicholas Moratelli^{1*} Davide Caffagni^{1*} Sara Sarto^{1*}

Lorenzo Baraldi¹ Marcella Cornia¹ Rita Cucchiara^{1,3}

¹University of Modena and Reggio Emilia, Italy ²University of Pisa, Italy ³IIT-CNR, Italy

¹{name.surname}@unimore.it ²{name.surname}@phd.unipi.it

Abstract

Recent progress in Multimodal Large Language Models (MLLMs) has highlighted the critical roles of both the visual backbone and the underlying language model. While prior work has primarily focused on scaling these components to billions of parameters, the trade-offs between model size, architecture, and performance remain under-explored. Additionally, inconsistencies in training data and evaluation protocols have hindered direct comparisons, making it difficult to derive optimal design choices. In this paper, we introduce LLaVA-MORE, a new family of MLLMs that integrates recent language models with diverse visual backbones. To ensure fair comparisons, we employ a unified training protocol applied consistently across all architectures. Our analysis systematically explores both small- and medium-scale LLMs – including Phi-4, LLaMA-3.1, and Gemma-2 – to evaluate multimodal reasoning, generation, and instruction following, while examining the relationship between model size and performance. Beyond evaluating the LLM impact on final results, we conduct a comprehensive study of various visual encoders, ranging from CLIP-based architectures to alternatives such as DINOv2, SigLIP, and SigLIP2. Additional experiments investigate the effects of increased image resolution and variations in pre-training datasets. Overall, our results provide insights into the design of more effective MLLMs, offering a reproducible evaluation framework that facilitates direct comparisons and can guide future model development. Our source code and trained models are publicly available at: <https://github.com/aimagelab/LLaVA-MORE>.

1. Introduction

The emergence of Large Language Models (LLMs) with remarkable expressive capabilities has revolutionized the way diverse language-related tasks are approached [1, 17, 61,

*Equal contribution.

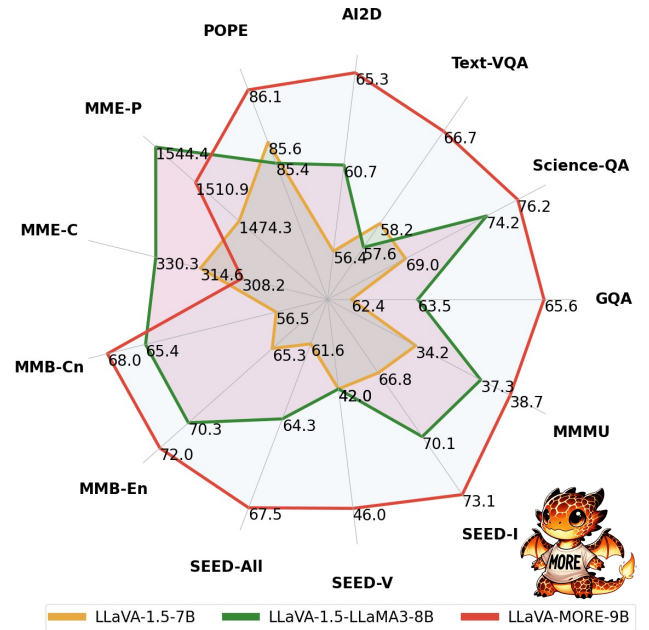


Figure 1. Performance comparison of the best version of LLaVA-MORE with other LLaVA variants across different benchmarks for multimodal reasoning and visual question answering.

64]. This advancement has inspired the Computer Vision and Multimedia communities to move beyond traditional text-only paradigms and adopt multiple modalities, including vision, audio, and beyond. Consequently, this shift has led to the emergence of Multimodal Large Language Models (MLLMs) [9], which establish sophisticated relationships between concepts across different embedding spaces, enabling richer multimodal understanding.

Current MLLMs [4, 5, 16, 26, 41, 42] typically integrate a language model with a visual backbone using specialized adapters that bridge the gap between modalities. While these systems demonstrate impressive performance, the field has converged around a somewhat narrow technical approach, with most implementations leveraging LLaMA-

derived LLMs and LLaVA-based training protocols. Additionally, visual encoders based on contrastive training such as CLIP [51] and its derivatives [21, 66, 71] have become the default choice for extracting visual features. These encoders are specifically trained to generate embeddings that seamlessly integrate with language models, further driving their widespread adoption. While contrastive learning has been highly effective in aligning images and text within a shared space, other vision models [10, 48] learn robust visual features in a purely self-supervised scheme, without relying on weak supervision from text. These models showcase intriguing emerging properties, and yet their application to MLLMs is relatively understudied.

To address this, our work conducts a comprehensive empirical study that systematically pairs diverse LLMs – ranging from efficient models [1] to significantly larger architectures [61, 64] – with various visual backbones [48, 51, 66, 71]. By exploring different architectural combinations, we aim to uncover the strengths and limitations of various vision-language integration strategies, shedding light on overlooked design choices and their impact on multimodal learning. Fig. 1 illustrates a comparison of our best-performing model (*i.e.*, LLaVA-MORE-9B, based on SigLIP2 as visual encoder and Gemma-2-9B as LLM) against LLaVA-based competitors (*i.e.*, LLaVA-1.5-7B [42] and LLaVA-1.5-LLaMA3-8B [53], both using a CLIP-based visual encoder and Vicuna-7B and LLaMA3-8B as LLM, respectively).

To ensure experimental consistency, we follow the established LLaVA [42] methodology, pre-training models on natural language description tasks before applying visual instruction fine-tuning to improve cross-domain generalization and human alignment. However, recent works not only introduce architectural enhancements but also incorporate specially curated datasets [7, 20, 44], making fair comparisons across models challenging. To isolate the role of data, in this work we compare LLaVA models pre-trained on different datasets against the same evaluation protocol.

To further explore the impact of training data, we conduct an additional study examining how different types of pre-training data influence multimodal alignment, reasoning ability, and generalization. Specifically, we compare models trained on web-scale image-text corpora, such as LAION [54], against those leveraging task-specific datasets with richer structural supervision [42]. Additionally, we explore the impact of using Recap-DataComp-1B [35], a recaptioned variant designed to enhance image-text alignment. Our results demonstrate that dataset selection significantly affects recognition capabilities and cross-domain transfer performance.

To summarize, this work provides key insights into cross-modal representation learning and offers a practical guide for developing more efficient and effective MLLMs,

while challenging conventional assumptions about visual and textual backbones and dataset requirements for optimizing pre-training strategies.

2. Related Works

Multimodal Large Language Models. The rapid advancements in language models, exemplified by GPT-4 [3] and Gemini [59], have transformed AI research, particularly through alignment techniques such as instruction tuning [50, 58] and reinforcement learning from human feedback [57]. Open-source LLMs [7, 17, 18, 27, 64] as well as more scale-efficient models [1, 2, 6, 61] have significantly driven innovation within the research community.

Building on these advancements, MLLMs extend traditional LLMs by incorporating visual perception capabilities, enabling models to process not only textual data but also interpret and reason about visual content. This integration significantly enhances their ability to tackle complex multimodal tasks [9]. A significant breakthrough in multimodal learning has come from the LLaVA models family [41, 42], which introduced visual instruction tuning to MLLMs. By leveraging a GPT-4-curated text-only dataset, LLaVA models effectively aligned visual and textual representations, leading to substantial improvements in multimodal performance. This approach has since become a foundational paradigm for training multimodal models, driving further advancements in the field.

Recent works have not only refined standard multimodal capabilities but also expanded their focus to a broader range of vision-centric benchmarks and diverse settings [7]. To achieve state-of-the-art results, some approaches prioritize enhancing the visual encoding phase, eventually fine-tuning [47] a vision encoder or even training it from scratch [4]. Others focus instead on scaling up spatial and temporal resolutions or improving visual token compression [8, 44] for better efficiency.

Despite the impressive performance of these models, a significant drawback lies in their reliance on specially curated datasets during training [7, 20, 31, 32, 44], which complicates fair evaluation and direct comparisons across different architectures and settings.

Large Language Models and Recent Advances. Despite the development of various LLM architectures [18, 52, 67, 69, 72], the LLaMA family [23, 64, 65] remains a popular choice thanks to its open-access nature, reliance on publicly available model weights, and availability in multiple sizes. Variants such as Alpaca [58] and Vicuna [17] further build upon LLaMA, enhancing its instruction-following and conversational abilities.

Recent research has focused on developing lightweight LLMs that strike a balance between efficiency and performance [6]. A notable example is the Gemma family [60, 61], which builds upon Gemini [59] and is designed

to provide strong reasoning and comprehension skills at various computational scales. Another significant contribution comes from the DeepSeek models [24, 39], which are characterized by their efficient training using reinforcement learning and their optimized inference processes.

A major breakthrough in LLM development is the introduction of LLaMA-3 [23], offering 8B to 405B parameter models with enhanced multilingual, coding, and reasoning abilities. Its improvements stem from rigorous data curation, pre-processing, and filtering, highlighting the critical role of high-quality training data in boosting efficiency and accuracy. This principle is further exemplified by the Phi models [1, 2, 36], which outperforms larger LLMs across multiple benchmarks. Among these, Phi-4 [1] pushes the boundaries of small-scale models through synthetic data generation, optimized training, and advanced post-training techniques, demonstrating that strategic data refinement can rival sheer model scaling.

Visual Backbones. Beyond advancements in language modeling, the visual backbone plays a crucial role in the performance of MLLMs by extracting and encoding image features for multimodal reasoning and understanding. The most widely used visual encoders are Vision Transformers (ViTs) trained with CLIP-style contrastive learning, with CLIP ViT-L [51] being the most commonly adopted architecture. Building on the success of CLIP, several studies have explored similar methodologies that leverage the inherent alignment of cross-modal embeddings.

The SigLIP family [66, 71] enhances CLIP by refining the training objective and filtering high-quality data, improving vision-language performance. Likewise, DINO models [10, 19, 48] introduces an automated pipeline for dataset filtering and rebalancing, leveraging vast collections of uncurated images to produce a diverse set of pre-trained visual models. Overall, stronger visual encoders generally boost MLLMs [34]. Expanding on this, some recent approaches [38, 40, 45, 62, 63] investigate multi-backbone fusion strategies, combining different encoders to enhance feature diversity and robustness. Other solutions, such as PaLI [14, 15], tackle the imbalance between visual and language parameters by scaling the vision backbone to billions of parameters. However, recent works [55] suggest that multi-scale feature extraction with smaller ViT-based models can outperform larger encoders, offering a more efficient alternative to scaling up visual encoders.

3. Overall Architecture

Following the LLaVA architecture, a typical MLLM consists of three fundamental components: a large language model backbone for user interaction and generating text, one or more visual encoders to process visual input and extract features, and at least one vision-to-language adapter to bridge the gap between visual and textual modalities [9].

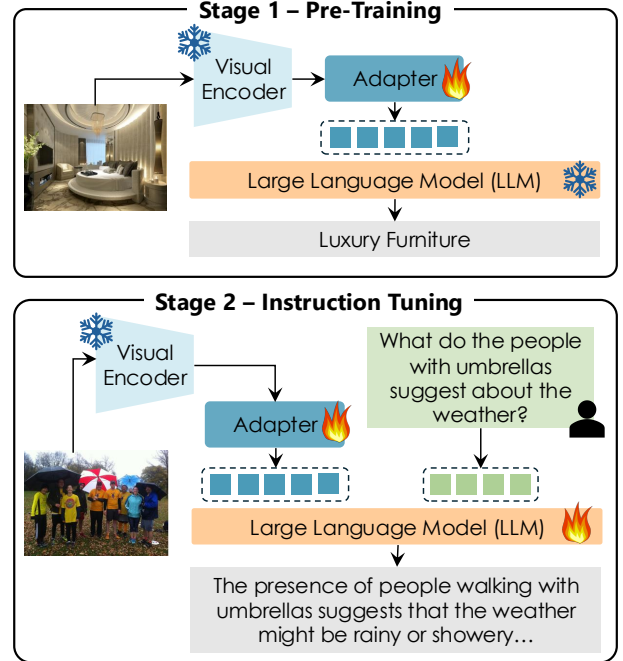


Figure 2. Overview of the LLaVA-MORE architecture. Our approach follows the standard LLaVA framework with a two-stage training process. The first stage aligns the visual features to the underlying LLM, ensuring effective cross-modal representation. The second stage enhances the MLLM conversational capabilities through visual instruction tuning. Following this paradigm, we systematically compare different LLM and visual encoder choices to evaluate their impact on various multimodal tasks.

The visual encoder provides essential global visual features to the LLM, with CLIP-based architectures [51, 68] being the most commonly used. In this setup, the visual encoder is typically pre-trained on another task and kept frozen for the entire training of the MLLM.

In this paper, we propose LLaVA-MORE, a new family of models that extend the standard LLaVA architecture by combining the visual encoder with various LLMs, ranging from small- to medium-scale models. As small-scale models, we utilize Gemma-2 2B [61] and Phi-4-Mini [1] (with 3.8B parameters), both designed for strong reasoning scalability, effectively challenging larger models. For medium-scale models, we select the variant of Gemma-2 [61] with 9B parameters alongside two recent architectures: the original LLaMA-3.1 [23] LLM with 8B parameters and its distilled DeepSeek-R1 version [24] (*i.e.*, DeepSeek-R1-Distill-LLaMA-8B). For each LLM category, we assess the impact of varying the visual backbone, with the aim to identify the optimal configuration. Specifically, our study compares the standard CLIP ViT-L/14 encoder employed in the LLaVA-1.5 model [42] with two variants of DINOv2 differentiated by the presence or the absence of visual register tokens [19, 48], known for their strong, semantically rich vi-

sual features, as well as SigLIP [71] and its more advanced successor, SigLIP2 [66].

To train our models, we follow the two-stage training paradigm commonly used in the literature. However, our approach stands out by applying a consistent training and evaluation strategy across all models, ensuring fairness in comparisons. In the first stage, only the vision-to-language adapter is optimized to align the image features with the text embedding space. In the second stage, visual instruction-following training is conducted to enhance multimodal conversational capabilities. During this phase, the parameters of both the multimodal adapter and the LLM are updated. An overview of the overall architecture and the two-stage training process is shown in Fig. 2.

4. Experimental Evaluation

4.1. Implementation Details

Architectural Components. The LLaVA-MORE family follows LLaVA architecture, employing CLIP ViT-L/14@336 as the visual backbone while varying the underlying language model. We categorize the selected LLMs into two groups based on scale: small-scale models, including Gemma-2-2B and Phi-4-3.8B, and medium-scale models, such as LLaMA-3.1-8B, DeepSeek-R1-Distill-LLaMA-8B, and Gemma-2-9B. To further investigate the impact of the visual backbone, we conduct experiments on the best-performing models, replacing CLIP [51] with alternative vision encoders, including DINOv2 [48], SigLIP [71], and SigLIP2 [66]. Additionally, we examine the effects of applying Scaling on Scales (S^2) [55] to both the CLIP and SigLIP2 architectures. Finally, motivated by the LLaVA-1.5 framework and insights from [12, 13], which highlight the advantages of using MLPs over linear projections in self-supervised learning, we adopt a two-layer MLP as the vision-language adapter to enhance multimodal fusion.

Training Details. Considering the LLaVA framework, we adopt a two-stage training strategy. In the first stage, only the weights of the adapter are updated using image-caption pairs as training data. Specifically, the caption style follows the alt-text structure as in web-scale multimodal datasets. The models are trained for one full epoch, covering a total of 558k samples from a combination of different sources (*i.e.*, LAION [54], CC3M [11], and SBU [49]). In the second step, we fine-tune the model on high-quality visual instruction-following data to improve its multimodal reasoning capabilities. This sequential training approach has been shown to significantly improve performance on downstream tasks [41]. Notably, the next token prediction is used as the loss function in both training phases. LLaVA-MORE models are trained with the same set of hyperparameters as LLaVA-1.5 to ensure consistency and comparability. In

particular, we employ a global batch size of 256 during pre-training and 128 during the visual instruction tuning phase. All experiments are run in a multi-GPU, multi-node configuration with a total of 16 A100 64GB NVIDIA GPUs.

4.2. Evaluation Benchmarks

We evaluate the LLaVA-MORE family on a diverse set of task-oriented and instruction-following benchmarks.

VQA Benchmarks. These primarily assess the model ability to answer questions based on visual inputs. For the VQA setting, we consider the following datasets:

- **GQA** [25] is based on Visual Genome scene graph annotations [29] and comprises 113k images and 22M questions focusing on scene understanding and compositionality. Results are reported on the test split, which represents 10% of the total image set.
- **ScienceQA** [46] evaluates models with challenging multimodal multiple-choice questions across three diverse domain subjects (*i.e.*, natural science, language science, and social science), 26 topics, 127 categories, and 379 skills. Each question is annotated with explanations linked to relevant lectures from elementary and high school science curricula. We report results on the test set which includes 4,241 examples.
- **TextVQA** [56] is a dataset built on Open Images [30] designed to evaluate the OCR capabilities of vision-and-language models. In our experiments, we employ the validation set which comprises 5,734 samples.
- **AI2D** [28] is a comprehensive collection of diagrams specifically designed for educational and research purposes. It consists of over 5,000 grade school science diagrams, which cover a wide range of topics and are accompanied by more than 15,000 diverse and richly formulated multiple-choice questions and answers.

MLLM Benchmarks. These evaluate broader multimodal language understanding and reasoning capabilities. Specifically, we consider the following benchmarks:

- **POPE** [37] is a benchmark for evaluating object hallucinations in MLLM generations. It includes several subsets, namely random, popular, and adversarial, which are generated using various sampling methodologies. The dataset consists of 8,910 binary classification queries, enabling thorough analysis of the object hallucination phenomena in MLLMs.
- **MME** [22] is designed to measure proficiency in various communication modalities through 14 diverse tasks. These tasks assess comprehension and manipulation in areas such as quantification, spatial reasoning, and color identification. Overall, it contains 2,374 samples.
- **MMBench (MMB)** [43] includes approximately 3,000 multiple-choice questions, distributed across a collection of 20 distinct domains and understanding capability. Questions are designed to assess the effectiveness

	VQA Benchmarks				MLLM Benchmarks								
	GQA	Science-QA	TextVQA	AI2D	POPE	MME-P	MME-C	MMB-Cn	MMB-En	SEED-AII	SEED-V	SEED-I	MMMU
<i>Small-Scale MLLMs</i>													
LLaVA-Phi-2.7B [73]	-	68.4	-	-	85.0	1335.1	-	-	59.8	-	-	-	-
LLaVA-MORE (Ours)													
Gemma-2-2B [61]	62.4	71.1	54.4	57.1	86.0	1401.1	337.8	65.8	53.3	62.2	41.9	67.6	33.4
Phi-4-3.8B [1]	62.1	71.3	54.0	61.1	85.9	1372.2	281.1	64.2	69.2	63.5	42.3	69.1	38.8
<i>Medium-Scale MLLMs</i>													
LLaVA-1.5-7B [42]	62.4	69.0	58.2	56.4	85.6	1474.3	314.6	56.5	65.3	61.6	42.0	66.8	34.2
LLaVA-1.5-LLaMA3-8B [53]	63.5	74.2	57.6	60.7	85.4	1544.4	330.3	65.4	70.3	64.3	42.0	70.1	37.3
LLaVA-MORE (Ours)													
LLaMA-3.1-8B [23]	63.6	76.3	58.4	61.8	85.1	1531.5	353.3	68.2	72.4	64.1	42.4	69.8	39.4
DeepSeek-R1-Distill-LLaMA-8B [24]	63.0	74.5	56.3	58.8	85.1	1495.1	295.0	66.8	61.3	63.5	43.5	68.6	38.1
Gemma-2-9B [61]	64.2	75.4	60.7	64.8	86.8	1522.5	307.5	65.9	71.9	64.5	44.1	69.9	37.9

Table 1. Performance analysis when changing the underlying LLMs. Results are reported considering both small- and medium-scale LLMs, comparing LLaVA-MORE with existing LLaVA-based variants. All models employ the CLIP ViT-L/14@336 as the visual backbone.

of MLLMs across various task paradigms. These capabilities are systematically structured into a hierarchical taxonomy, encompassing broad categories like perception and reasoning, as well as finer-grained skills such as object localization and attribute inference.

- **SEED-Bench (SEED)** [33] evaluates MLLMs across 12 dimensions, including scene understanding, OCR, and action recognition. The dataset comprises 19k multiple-choice questions curated by human annotators.
- **MMMU** [70] is a challenging benchmark for multimodal models, focusing on massive multi-discipline tasks demanding college-level subject knowledge. It consists of 900 validation samples drawn from university textbooks or online courses spanning six main disciplines. Questions may include multiple images interleaved with text. Evaluation includes exact and word matching for multiple-choice and open-ended questions, and models are tested in zero or few-shot settings.

4.3. Assessing the Optimal LLM Choice

LLaVA-MORE extends the widely recognized LLaVA architecture by incorporating small- and medium-scale LLMs. As shown in Table 1, our experiments first investigate the relationship between model size and performance across various benchmarks. Among the small-scale LLMs, we compare the LLaVA version based on Phi-2.7B [73] with our versions based on Phi-4-3.8B and Gemma-2-2B. Notably, both versions of LLaVA-MORE consistently outperform the existing baseline across multiple benchmarks. Notably, Phi-4-3.8B achieves the highest scores on most benchmarks, particularly excelling in the MMMU performance, where it surpasses Gemma-2-2B by 5.4%. Similar improvements are also evident in the SEED dataset, where Phi4-3.8B achieved significantly higher performance than other small-scale LLMs. These results underscore Phi-4-3.8B’s superior reasoning and generalization capabilities.

Conversely, among medium-scale models, LLaVA-1.5-7B and LLaVA-1.5-LLaMA3-8B provide stronger base-

lines, with LLaVA-1.5-LLaMA3-8B achieving the highest score in MME-P (1544.4). However, our LLaVA-MORE models consistently surpass these baselines, demonstrating superior performance across both VQA and MLLM benchmarks. In particular, Gemma-2-9B emerges as the best-performing model, especially excelling in VQA benchmarks. It achieves the highest scores on GQA and AI2D, significantly outperforming both baselines and other models within the LLaVA-MORE family. In MLLM benchmarks, LLaVA-MORE combined with LLaMA-3.1-8B demonstrates instead strong capabilities on the MMB dataset, showing good results in multiple-choice question settings. Notably, our models exhibit less sensitivity to object hallucinations, as seen by the results achieved on the POPE benchmark, and demonstrate superior performance on the SEED dataset, further highlighting their robustness in multimodal reasoning tasks.

Comparing small- and medium-scale models, it is noteworthy that some small-scale LLaVA-MORE models outperform even medium-scale baselines like LLaVA-1.5-7B. For instance, in Science-QA and AI2D, LLaVA-MORE with Phi-4-3.8B surpasses both the baseline and LLaVA-MORE with DeepSeek-R1-Distill-LLaMA-8B.

This trend extends to MLLM benchmarks, where LLaVA-MORE models demonstrate competitive performance in MMB and SEED, further highlighting their efficiency and strong reasoning capabilities despite their smaller size. Overall, our results emphasize that scaling up is not the only path to better performance, as architectural choices and fine-tuning strategies significantly impact model effectiveness across different benchmarks.

Open Problems

Multimodal reasoning needs improvement through training strategies specifically designed for cross-modal understanding.

💡 Key Takeaway 1

Recent small-scale models are comparable to medium-scale models of the previous generation.

4.4. Changing the Visual Backbone

We then investigate which visual backbone is more promising for building MLLMs. To this end, we select the best small- and medium-scale models resulting from Table 1 and study how their performance is affected when the visual encoder is varied. In detail, we opt for Phi-4-3.8B as the small-scale LLM (*i.e.*, LLaVA-MORE-3.8B), and Gemma-2-9B as the medium-scale one (*i.e.*, LLaVA-MORE-9B). As per the visual backbone, in Table 2, we include four pre-trained ViT-based models, in addition to the standard CLIP used by LLaVA. All models share the ViT-L/14 architecture, and yet there are striking differences in terms of training data, input image resolutions, and on the pre-training strategies. In particular, we can delineate two pre-training paradigms: DINOv2 [48], eventually enhanced with registers [19], has been pre-trained with self-supervision and knowledge distillation on 142M images, while the other visual encoders leverage the weak supervision of noisy image-text pairs during pre-training. Specifically, CLIP [51] learns robust visual models via contrastive learning, while SigLIP [71] exploits the sigmoid loss to improve cross-modal alignment. The recent SigLIP2 [66] builds upon SigLIP by incorporating additional training objectives, including image captioning, self-distillation, and image-masked prediction.

From Table 2, we observe that image-text pre-trained visual backbones consistently outperform DINOv2 backbones at both small and medium scales. Moreover, adding register tokens in DINOv2 does not help in reducing the gap. We retain that, thanks to their pre-training, CLIP and SigLIP provide visual features that are readily aligned with text, simplifying the role of the multimodal adapter of making them understandable by the LLM.

The only exception is MME-C, where DINOv2 with registers scores the highest at the 3.8B scale, and DINOv2 is the best at the 9B scale with 334.3 points. Among the models that benefited from image-text pre-training, SigLIP shows a substantial improvement over CLIP at both scales, highlighting its effectiveness despite introducing a computational overhead—specifically, it forces the LLM to process approximately 26% more visual tokens due to the use of higher-resolution inputs. Despite its more complicated training recipe, the new SigLIP2 performs on par with the original SigLIP at the 3.8B scale but records an average 0.4% gain over SigLIP at the 9B scale. For this reason, we will always include SigLIP2 as the visual backbone in all the subsequent experiments. One key finding from our evaluation is that SigLIP-based visual backbones establish

a new performance frontier for MLLMs across most benchmarks. Beyond the advantage conferred by increased resolution, we attribute much of this success to the massive billion-scale image-text pre-training enabled by the sigmoid loss of SigLIP, compared to the 400M image-text pairs seen by CLIP during pre-training.

💡 Key Takeaway 2

Visual backbones trained with contrastive learning outperform self-supervised visual encoders.

💡 Key Takeaway 3

Different versions of SigLIP consistently outperform other visual backbones.

4.5. Changing the Image Resolution

The choice of a robust visual backbone and the appropriate LLM are critical factors in enhancing model performance. However, the resolution of the input image plays a similarly important role in visual understanding. Higher image resolutions provide more fine-grained visual information, which can significantly aid the MLLM in better interpreting the content and thereby improving performance.

Table 3 presents an evaluation of the LLaVA-MORE models that analyzes the impact of increasing image resolution when using the CLIP and SigLIP2 visual backbones. To tackle this, we leverage the S^2 scheme [55], a widely adopted method designed to enhance image resolution. Specifically, we interpolate the input image to create additional copies with $2\times$ and $3\times$ the standard resolution accepted by the visual encoder. The copies are chunked into 4 and 9 squared images respectively, of the same resolution as the original one. In total, 14 images are generated per sample, each processed independently by the visual encoder. The resulting visual tokens are spatially pooled and then channel-wise concatenated, resulting in the same number of visual tokens, but with $3\times$ more channels.

Notably, from Table 3 (top), it can be seen that S^2 generally improves LLaVA-MORE-3.8B when using CLIP as the visual backbone. The improvements are even more consistent when switching to SigLIP2, which already works at a higher resolution than CLIP. However, when scaling up to LLaVA-MORE-9B (Table 3 bottom), the benefits of S^2 vanish for some benchmarks. For instance, on Science-QA and AI2D, S^2 appears detrimental at the 9B scale, while it is advantageous with LLaVA-MORE-3.8B.

From these results, we can conclude that small-scale MLLMs may greatly benefit from working with high-resolution images. However, the positive impact of higher resolution appears to diminish as model size increases, and,

		VQA Benchmarks					MLLM Benchmarks								
	Resolution	# Tokens	GQA	Science-QA	TextVQA	AI2D	POPE	MME-P	MME-C	MMB-Cn	MMB-En	SEED-All	SEED-V	SEED-I	MMMU
LLaVA-MORE-3.8B (Ours)															
CLIP ViT-L/14 [51]	336 ²	576	62.1	71.3	54.0	61.1	85.9	1372.2	281.1	64.2	69.2	63.5	42.3	69.1	38.8
DINOv2 ViT-L/14 [48]	224 ²	256	60.9	66.6	41.4	58.2	85.5	1236.6	281.1	53.8	58.9	59.8	40.6	64.8	37.9
DINOv2 _{reg} ViT-L/14 [19]	224 ²	256	60.4	69.0	41.3	56.4	85.2	1263.2	288.2	57.4	51.4	58.7	41.4	63.2	38.6
SigLIP ViT-L/14 [71]	384 ²	729	63.6	73.8	57.6	62.9	86.4	1379.0	282.9	66.5	71.4	65.7	46.4	70.8	40.0
SigLIP2 ViT-L/14 [66]	384 ²	729	63.4	71.8	59.7	62.9	86.5	1406.7	282.5	66.8	69.8	66.4	47.4	71.4	38.8
LLaVA-MORE-9B (Ours)															
CLIP ViT-L/14 [51]	336 ²	576	64.2	75.4	60.7	64.8	86.8	1522.5	307.5	65.9	71.9	64.5	44.1	69.9	37.9
DINOv2 ViT-L/14 [48]	224 ²	256	63.1	71.5	48.1	61.3	85.3	1394.4	334.3	56.4	63.8	61.0	40.6	66.4	38.7
DINOv2 _{reg} ViT-L/14 [19]	224 ²	256	62.8	69.1	47.9	59.1	84.0	1413.9	295.4	60.1	53.8	60.1	42.3	64.7	38.3
SigLIP ViT-L/14 [71]	384 ²	729	64.8	76.3	63.9	64.7	86.1	1487.9	299.3	69.1	74.4	66.6	46.6	71.9	39.7
SigLIP2 ViT-L/14 [66]	384 ²	729	65.6	76.2	66.7	65.3	86.1	1510.9	308.2	68.0	72.0	67.5	46.0	73.1	38.7

Table 2. Performance analysis with varying visual backbones. Results are reported for the best small- and medium-scale LLaVA-MORE configurations using Phi-4-3.8B and Gemma-2-9B, respectively. Input resolution and the number of visual tokens are also included.

		VQA Benchmarks					MLLM Benchmarks									
	S ²	Resolution	# Tokens	GQA	Science-QA	TextVQA	AI2D	POPE	MME-P	MME-C	MMB-Cn	MMB-En	SEED-All	SEED-V	SEED-I	MMMU
LLaVA-MORE-3.8B (Ours)																
CLIP ViT-L/14 [51]	✗	336 ²	576	62.1	71.3	54.0	61.1	85.9	1372.2	281.1	64.2	69.2	63.5	42.3	69.1	38.8
CLIP ViT-L/14 [55]	✓	336 ² ×14	576	62.7	71.8	54.9	61.7	86.9	1366.8	263.9	68.6	64.4	64.2	43.1	69.8	39.8
SigLIP2 ViT-L/14 [66]	✗	384 ²	729	63.4	71.8	59.7	62.9	86.5	1406.7	282.5	66.8	69.8	66.4	47.4	71.4	38.8
SigLIP2 ViT-L/14 [55]	✓	384 ² ×14	729	64.1	72.2	61.5	63.2	87.4	1466.7	331.1	69.2	70.7	67.0	47.6	72.1	38.7
LLaVA-MORE-9B (Ours)																
CLIP ViT-L/14 [51]	✗	336 ²	576	64.2	75.4	60.7	64.8	86.8	1522.5	307.5	65.9	71.9	64.5	44.1	69.9	37.9
CLIP ViT-L/14 [55]	✓	336 ² ×14	576	65.2	73.7	63.4	64.2	86.1	1495.9	331.8	68.6	70.2	65.1	45.2	70.4	39.0
SigLIP2 ViT-L/14 [66]	✗	384 ²	729	65.6	76.2	66.7	65.3	86.1	1510.9	308.2	68.0	72.0	67.5	46.0	73.1	38.7
SigLIP2 ViT-L/14 [55]	✓	384 ² ×14	729	65.9	74.9	68.1	64.1	86.7	1557.6	320.7	68.6	73.5	67.2	45.6	72.9	40.2

Table 3. Performance analysis when applying the S² multi-scale visual processing [55]. Results are reported considering the best small- and medium-scale LLaVA-MORE configurations with Phi-4-3.8B and Gemma-2-9B, using both CLIP and SigLIP2 visual encoders.

ultimately, the benefits of increasing image resolution seem to be highly task-dependent. For instance, with TextVQA, a benchmark that heavily relies on detecting and recognizing text within images, S² consistently brings improvements. A similar pattern is found on GQA, which challenges MLLMs with questions requiring in-depth scene understanding. Curiously, we find substantial gains by applying S² on the Chinese version of MMBench (MMB-Cn), especially at the 3.8B scale, while its behavior on the English version is conflicting: S² improves with SigLIP2, but it is detrimental with CLIP.

Key Takeaway 4

Input resolution and number of visual tokens are critical to achieving good results in multimodal benchmarks, especially with small-scale models.

4.6. Dataset Contribution During Pre-Training

Finally, we analyze the effect of using different data sources for the pre-training phase. Specifically, we select 558K samples from three different sources for image-caption pairs: (i) samples directly derived from the LAION dataset, (ii) samples from Recap-DataComp-1B [35] where captions

are generated by an MLLM and provide a dense description of the scene, and (iii) a balanced combination of the first two configurations (*i.e.*, LAION+Recap). Table 4 compares these three new datasets against the original LLaVA pre-training recipe (*i.e.*, LLaVA Pre-Train LCS), consisting of a mixture of image-caption pairs from LAION [54], CC3M [11], and SBU [49].

Interestingly, LLaVA-MORE-3.8B never achieves the top score with the original mixture. Conversely, exclusively training on LAION stands out as the winning choice in 8 out of 13 benchmarks. This may be because LAION’s noisy web-sourced pairs closely resemble the nature of the training data used by the SigLIP2 visual encoder behind LLaVA-MORE-3.8B. In contrast, LLaVA-MORE-9B shows more robust performance across the different configurations. Notably, adding Recap samples boosts LLaVA-MORE-9B’s Chinese fluency, leading to the best score of 69.4 on MMB-Cn and improving other MLLM results.

Key Takeaway 5

The source of pre-training data plays a role at small scales, but it does not significantly impact medium-scale models.

	VQA Benchmarks				MLLM Benchmarks								
	GQA	Science-QA	TextVQA	AI2D	POPE	MME-P	MME-C	MMB-Cn	MMB-En	SEED-AII	SEED-V	SEED-I	MMMU
LLaVA-MORE-3.8B (Ours)													
LLaVA Pre-Train LCS (558k)	63.4	71.8	59.7	62.9	86.5	1406.7	282.5	66.8	69.8	66.4	47.4	71.4	38.8
LAION (558k)	64.3	72.5	62.3	65.2	86.8	1453.2	287.1	67.2	72.3	66.6	46.4	71.9	39.7
Recap (558k)	64.6	71.7	61.4	64.5	86.5	1428.7	297.9	67.1	71.6	67.3	47.7	72.5	39.0
LAION+Recap (558k)	64.6	71.8	61.3	63.9	86.6	1425.8	297.5	65.8	71.7	67.6	47.5	72.9	39.2
LLaVA-MORE-9B (Ours)													
LLaVA Pre-Train LCS (558k)	65.6	76.2	66.7	65.3	86.1	1510.9	308.2	68.0	72.0	67.5	46.0	73.1	38.7
LAION (558k)	65.6	76.0	67.0	65.1	86.9	1579.8	350.7	68.5	73.9	67.4	45.4	73.2	41.1
Recap (558k)	65.9	76.2	67.2	64.3	86.9	1540.8	318.2	69.4	74.7	67.6	47.2	73.0	40.2
LAION+Recap (558k)	65.8	77.1	67.8	65.2	86.7	1537.8	335.4	65.9	73.5	67.4	45.2	73.1	41.2

Table 4. Performance analysis when changing the training dataset during the first pre-training stage. Results are reported for the best small- and medium-scale LLaVA-MORE configurations using Phi-4-3.8B and Gemma-2-9B.



LLaVA-1.5-7B: The image captures a thrilling moment of a skier in mid-air, jumping off a snowy hill. The skier is skillfully performing a jump, showcasing their athleticism and control. The skis are visible beneath the skier, indicating their position in the air. The scene takes place in a mountainous area, with the skier surrounded by snow-covered terrain. The skier's jump is the main focus of the image, emphasizing the excitement and adrenaline rush associated with this winter sport.

LLaVA-MORE-3.8B: The image captures a thrilling moment of a snowboarder in mid-air, performing a jump off a snowy hill. The snowboarder is skillfully flying through the air, showcasing their impressive abilities. In the scene, there are several trees scattered around the area, adding to the natural beauty of the snowy landscape. The snowboarder is the main focus of the image, with the trees providing a picturesque backdrop for their daring stunt.

LLaVA-MORE-9B: In the image, a person is snowboarding down a snow-covered slope, performing a jump and flying through the air. The snowboarder is wearing a red and white jacket, and their snowboard is visible beneath them as they soar through the air. The scene captures the excitement and skill of the snowboarder as they execute this impressive aerial maneuver.

Figure 3. Qualitative of image descriptions generated by three MLLMs (LLaVA-1.5-7B, LLaVA-MORE-3.8B, and LLaVA-MORE-9B). The example shows differences in detail, context, and narrative style across scenarios like sports, transport, toys, and portraits.

4.7. Qualitative Results

To better understand the behavior of different MLLMs beyond their quantitative performance on standard MLLM and VQA benchmarks, we also present qualitative results on the image captioning task¹, as shown in Fig. 3. In particular, we compare LLaVA-1.5-7B [42], which serves as our baseline, against our model based on Phi-4-3.8B and Gemma-2-9B using SigLip2 as visual encoder. As it can be seen, LLaVA-MORE versions can effectively describe input images and provide detailed and rich textual descriptions. For example, only the two versions of LLaVA-MORE successfully avoid hallucinations and provide an accurate description of the scene. In contrast, the LLaVA-1.5-7B model incorrectly identifies the object in question (*i.e.*, erroneously recognizing the snowboard in the image as skis) highlighting a notable failure in visual understanding and alignment with textual output.

Key Takeaway 6

No single model configuration consistently outperforms others across all experiments. Performance highly depends on the specific task.

¹For these qualitative results, we use the prompt: "Describe this image."

5. Conclusion

This work presents a quantitative analysis of the integration of different LLMs and visual backbones into the LLaVA architecture, aiming to systematically and comparably evaluate the contribution of each component. To the best of our knowledge, this is the first comparative analysis of different backbones conducted under consistent experimental settings, using the same dataset across all training stages and the same evaluation protocol. Moreover, this work also aims to develop a framework for training and evaluating different versions of MLLM. To support this, we will release the code along with the model checkpoints to encourage the community to experiment with new configurations.

Limitations

In this work, an analysis of a subset of publicly available LLMs and visual backbones was considered. The rapid evolution of this research area means that the results presented provide a snapshot of the best configurations currently achievable. In addition, preliminary results are presented on the integration of text-only reasoning models into multimodal tasks through fine-tuning. These insights can serve as a starting point to bridge the gap between text-only and multimodal reasoning.

Acknowledgments

We acknowledge the CINECA award under the ISCRA initiative, for the availability of high-performance computing resources. This work has been conducted under two research grants, one co-funded by Leonardo S.p.A. and the other co-funded by Altilia s.r.l., and supported by the PNRR-M4C2 project “FAIR - Future Artificial Intelligence Research” and by the PNRR project “IT-SERR - Italian Strengthening of Esfri RI Resilience” (CUP B53C22001770006), both funded by the European Union - NextGenerationEU.

References

- [1] Marah Abidin, Jyoti Aneja, Harkirat Behl, Sébastien Bubeck, Ronen Eldan, Suriya Gunasekar, Michael Harrison, Russell J Hewett, Mojan Javaheripi, Piero Kauffmann, et al. Phi-4 Technical Report. *arXiv preprint arXiv:2412.08905*, 2024. 1, 2, 3, 5
- [2] Abdelrahman Abouelenin, Atabak Ashfaq, Adam Atkinson, Hany Awadalla, Nguyen Bach, Jianmin Bao, Alon Benham, Martin Cai, Vishrav Chaudhary, Congcong Chen, et al. Phi-4-Mini Technical Report: Compact yet Powerful Multimodal Language Models via Mixture-of-LoRAs. *arXiv preprint arXiv:2503.01743*, 2025. 2, 3
- [3] Josh Achiam, Steven Adler, Sandhini Agarwal, Lama Ahmad, Ilge Akkaya, Florencia Leoni Aleman, Diogo Almeida, Janko Altschmidt, Sam Altman, Shyamal Anadkat, et al. GPT-4 Technical Report. *arXiv preprint arXiv:2303.08774*, 2023. 2
- [4] Praveesh Agrawal, Szymon Antoniak, Emma Bou Hanna, Baptiste Bout, Devendra Chaplot, Jessica Chudnovsky, Diogo Costa, Baudouin De Monicault, Saurabh Garg, Theophile Gervet, et al. Pixtral 12b. *arXiv preprint arXiv:2410.07073*, 2024. 1, 2
- [5] Jean-Baptiste Alayrac, Jeff Donahue, Pauline Luc, Antoine Miech, Iain Barr, Yana Hasson, Karel Lenc, Arthur Mensch, Katherine Millican, Malcolm Reynolds, et al. Flamingo: a visual language model for few-shot learning. In *NeurIPS*, 2022. 1
- [6] Loubna Ben Allal, Anton Lozhkov, Elie Bakouch, Gabriel Martín Blázquez, Guilherme Penedo, Lewis Tunstall, Andrés Marafioti, Hynek Kydlíček, Agustín Piqueres Lajarín, Vaibhav Srivastav, et al. SmolLM2: When Smol Goes Big—Data-Centric Training of a Small Language Model. *arXiv preprint arXiv:2502.02737*, 2025. 2
- [7] Jinze Bai, Shuai Bai, Yunfei Chu, Zeyu Cui, Kai Dang, Xiaodong Deng, Yang Fan, Wenbin Ge, Yu Han, Fei Huang, et al. Qwen Technical Report. *arXiv preprint arXiv:2309.16609*, 2023. 2
- [8] Daniel Bolya, Cheng-Yang Fu, Xiaoliang Dai, Peizhao Zhang, Christoph Feichtenhofer, and Judy Hoffman. Token Merging: Your ViT but Faster. In *ICLR*, 2023. 2
- [9] Davide Caffagni, Federico Cocchi, Luca Barsellotti, Nicholas Moratelli, Sara Sarto, Lorenzo Baraldi, Lorenzo Baraldi, Marcella Cornia, and Rita Cucchiara. The Revolution of Multimodal Large Language Models: A Survey. In *ACL Findings*, 2024. 1, 2, 3
- [10] Mathilde Caron, Hugo Touvron, Ishan Misra, Hervé Jégou, Julien Mairal, Piotr Bojanowski, and Armand Joulin. Emerging Properties in Self-Supervised Vision Transformers. In *ICCV*, 2021. 2, 3
- [11] Soravit Changpinyo, Piyush Sharma, Nan Ding, and Radu Soricut. Conceptual 12M: Pushing Web-Scale Image-Text Pre-Training To Recognize Long-Tail Visual Concepts. In *CVPR*, 2021. 4, 7
- [12] Ting Chen, Simon Kornblith, Mohammad Norouzi, and Geoffrey Hinton. A Simple Framework for Contrastive Learning of Visual Representations. In *ICML*, 2020. 4
- [13] Xinlei Chen, Haoqi Fan, Ross Girshick, and Kaiming He. Improved Baselines with Momentum Contrastive Learning. *arXiv preprint arXiv:2003.04297*, 2020. 4
- [14] Xi Chen, Josip Djolonga, Piotr Padlewski, Basil Mustafa, Soravit Changpinyo, Jialin Wu, Carlos Riquelme Ruiz, Sebastian Goodman, Xiao Wang, Yi Tay, et al. PaLI-X: On Scaling up a Multilingual Vision and Language Model. *arXiv preprint arXiv:2305.18565*, 2023. 3
- [15] Xi Chen, Xiao Wang, Soravit Changpinyo, AJ Piergiovanni, Piotr Padlewski, Daniel Salz, Sebastian Goodman, Adam Grycner, Basil Mustafa, Lucas Beyer, et al. PaLI: A Jointly-Scaled Multilingual Language-Image Model. In *ICLR*, 2023. 3
- [16] Zhe Chen, Jiannan Wu, Wenhai Wang, Weijie Su, Guo Chen, Sen Xing, Muyan Zhong, Qinglong Zhang, Xizhou Zhu, Lewei Lu, et al. Internvl: Scaling up vision foundation models and aligning for generic visual-linguistic tasks. In *CVPR*, 2024. 1
- [17] Wei-Lin Chiang, Zhuohan Li, Zi Lin, Ying Sheng, Zhanghao Wu, Hao Zhang, Lianmin Zheng, Siyuan Zhuang, Yonghao Zhuang, Joseph E. Gonzalez, Ion Stoica, and Eric P. Xing. Vicuna: An Open-Source Chatbot Impressing GPT-4 with 90%* ChatGPT Quality, 2023. 1, 2
- [18] Hyung Won Chung, Le Hou, Shayne Longpre, Barret Zoph, Yi Tay, William Fedus, Yunxuan Li, Xuezhi Wang, Mostafa Dehghani, Siddhartha Brahma, et al. Scaling Instruction-Finetuned Language Models. *JMLR*, 25(70):1–53, 2024. 2
- [19] Timothée Darcet, Maxime Oquab, Julien Mairal, and Piotr Bojanowski. Vision Transformers Need Registers. In *ICLR*, 2024. 3, 6, 7
- [20] Matt Deitke, Christopher Clark, Sangho Lee, Rohun Tripathi, Yue Yang, Jae Sung Park, Mohammadreza Salehi, Niklas Muennighoff, Kyle Lo, Luca Soldaini, et al. Molmo and PixMo: Open Weights and Open Data for State-of-the-Art Vision-Language Models. *arXiv preprint arXiv:2409.17146*, 2024. 2
- [21] Yuxin Fang, Wen Wang, Binhui Xie, Quan Sun, Ledell Wu, Xinggang Wang, Tiejun Huang, Xinlong Wang, and Yue Cao. EVA: Exploring the Limits of Masked Visual Representation Learning at Scale. In *CVPR*, 2023. 2
- [22] Chaoyou Fu, Peixian Chen, Yunhang Shen, Yulei Qin, Mengdan Zhang, Xu Lin, Jinrui Yang, Xiawu Zheng, Ke Li, Xing Sun, et al. MME: A Comprehensive Evaluation Benchmark for Multimodal Large Language Models. *arXiv preprint arXiv:2306.13394*, 2023. 4

- [23] Aaron Grattafiori, Abhimanyu Dubey, Abhinav Jauhri, Abhinav Pandey, Abhishek Kadian, Ahmad Al-Dahle, Aiesha Letman, Akhil Mathur, Alan Schelten, Alex Vaughan, et al. The Llama 3 Herd of Models. *arXiv preprint arXiv:2407.21783*, 2024. 2, 3, 5
- [24] Daya Guo, Dejian Yang, Haowei Zhang, Junxiao Song, Ruoyu Zhang, Runxin Xu, Qihao Zhu, Shirong Ma, Peiyi Wang, Xiao Bi, et al. DeepSeek-R1: Incentivizing Reasoning Capability in LLMs via Reinforcement Learning. *arXiv preprint arXiv:2501.12948*, 2025. 3, 5
- [25] Drew A Hudson and Christopher D Manning. GQA: A New Dataset for Real-World Visual Reasoning and Compositional Question Answering. In *CVPR*, 2019. 4
- [26] Dongfu Jiang, Xuan He, Huaye Zeng, Cong Wei, Max Ku, Qian Liu, and Wenhu Chen. MANTIS: Interleaved Multi-Image Instruction Tuning. *arXiv preprint arXiv:2405.01483*, 2024. 1
- [27] Fengqing Jiang, Zhangchen Xu, Luyao Niu, Boxin Wang, Jinyuan Jia, Bo Li, and Radha Poovendran. Identifying and Mitigating Vulnerabilities in LLM-Integrated Applications. In *NeurIPS Workshops*, 2023. 2
- [28] Aniruddha Kembhavi, Mike Salvato, Eric Kolve, Minjoon Seo, Hannaneh Hajishirzi, and Ali Farhadi. A diagram is worth a dozen images. In *ECCV*, 2016. 4
- [29] Ranjay Krishna, Yuke Zhu, Oliver Groth, Justin Johnson, Kenji Hata, Joshua Kravitz, Stephanie Chen, Yannis Kalantidis, Li-Jia Li, David A Shamma, et al. Visual Genome: Connecting Language and Vision Using Crowd-sourced Dense Image Annotations. *IJCV*, 123:32–73, 2017. 4
- [30] Alina Kuznetsova, Hassan Rom, Neil Alldrin, Jasper Uijlings, Ivan Krasin, Jordi Pont-Tuset, Shahab Kamali, Stefan Popov, Matteo Mallocci, Alexander Kolesnikov, et al. The Open Images Dataset V4: Unified Image Classification, Object Detection, and Visual Relationship Detection at Scale. *IJCV*, 128:1956–1981, 2020. 4
- [31] Hugo Laurençon, Lucile Saulnier, Léo Tronchon, Stas Bekman, Amanpreet Singh, Anton Lozhkov, Thomas Wang, Siddharth Karamcheti, Alexander Rush, Douwe Kiela, et al. OBELICS: An Open Web-Scale Filtered Dataset of Interleaved Image-Text Documents. In *NeurIPS*, 2023. 2
- [32] Hugo Laurençon, Léo Tronchon, Matthieu Cord, and Victor Sanh. What matters when building vision-language models? In *NeurIPS*, 2024. 2
- [33] Bohao Li, Rui Wang, Guangzhi Wang, Yuying Ge, Yixiao Ge, and Ying Shan. SEED-Bench: Benchmarking Multimodal LLMs with Generative Comprehension. *arXiv preprint arXiv:2307.16125*, 2023. 5
- [34] Junnan Li, Dongxu Li, Silvio Savarese, and Steven Hoi. BLIP-2: Bootstrapping Language-Image Pre-training with Frozen Image Encoders and Large Language Models. In *ICML*, 2023. 3
- [35] Xianhang Li, Haoqin Tu, Mude Hui, Zeyu Wang, Bingchen Zhao, Junfei Xiao, Sucheng Ren, Jieru Mei, Qing Liu, Huangjie Zheng, et al. What If We Recaption Billions of Web Images with LLaMA-3? In *CVPR Workshops*, 2024. 2, 7
- [36] Yuanzhi Li, Sébastien Bubeck, Ronen Eldan, Allie Del Giorno, Suriya Gunasekar, and Yin Tat Lee. Textbooks Are All You Need II: phi-1.5 technical report. *arXiv preprint arXiv:2309.05463*, 2023. 3
- [37] Yifan Li, Yifan Du, Kun Zhou, Jinpeng Wang, Wayne Xin Zhao, and Ji-Rong Wen. Evaluating Object Hallucination in Large Vision-Language Models. In *EMNLP*, 2023. 4
- [38] Ziyi Lin, Chris Liu, Renrui Zhang, Peng Gao, Longtian Qiu, Han Xiao, Han Qiu, Chen Lin, Wenqi Shao, Keqin Chen, et al. SPHINX: The Joint Mixing of Weights, Tasks, and Visual Embeddings for Multi-modal Large Language Models. *arXiv preprint arXiv:2311.07575*, 2023. 3
- [39] Aixiu Liu, Bei Feng, Bin Wang, Bingxuan Wang, Bo Liu, Chenggang Zhao, Chengqi Deng, Chong Ruan, Damai Dai, Daya Guo, et al. DeepSeek-V2: A Strong, Economical, and Efficient Mixture-of-Experts Language Model. *arXiv preprint arXiv:2405.04434*, 2024. 3
- [40] Dongyang Liu, Renrui Zhang, Longtian Qiu, Siyuan Huang, Weifeng Lin, Shitian Zhao, Shijie Geng, Ziyi Lin, Peng Jin, Kaipeng Zhang, et al. SPHINX-X: Scaling Data and Parameters for a Family of Multi-modal Large Language Models. In *ICML*, 2024. 3
- [41] Haotian Liu, Chunyuan Li, Qingyang Wu, and Yong Jae Lee. Visual Instruction Tuning. In *NeurIPS*, 2023. 1, 2, 4
- [42] Haotian Liu, Chunyuan Li, Yuheng Li, and Yong Jae Lee. Improved baselines with visual instruction tuning. In *CVPR*, 2024. 1, 2, 3, 5, 8
- [43] Yuan Liu, Haodong Duan, Yuanhan Zhang, Bo Li, Songyang Zhang, Wangbo Zhao, Yike Yuan, Jiaqi Wang, Conghui He, Ziwei Liu, et al. MMBench: Is Your Multi-modal Model an All-around Player? In *ECCV*, 2024. 4
- [44] Zhijian Liu, Ligeng Zhu, Baifeng Shi, Zhuoyang Zhang, Yuming Lou, Shang Yang, Haocheng Xi, Shiyi Cao, Yuxian Gu, Dacheng Li, et al. NVILA: Efficient frontier visual language models. *arXiv preprint arXiv:2412.04468*, 2024. 2
- [45] Haoyu Lu, Wen Liu, Bo Zhang, Bingxuan Wang, Kai Dong, Bo Liu, Jingxiang Sun, Tongzheng Ren, et al. DeepSeek-VL: Towards Real-World Vision-Language Understanding. *arXiv preprint arXiv:2403.05525*, 2024. 3
- [46] Pan Lu, Swaroop Mishra, Tanglin Xia, Liang Qiu, Kai-Wei Chang, Song-Chun Zhu, Oyvind Tafjord, Peter Clark, and Ashwin Kalyan. Learn to Explain: Multimodal Reasoning via Thought Chains for Science Question Answering. In *NeurIPS*, 2022. 4
- [47] Brandon McKinzie, Zhe Gan, Jean-Philippe Fauconnier, Sam Dodge, Bowen Zhang, Philipp Duffer, Dhruvi Shah, Xianzhi Du, Futang Peng, Anton Belyi, et al. MM1: Methods, Analysis and Insights from Multimodal LLM Pre-Training. In *ECCV*, 2024. 2
- [48] Maxime Oquab, Timothée Darcet, Théo Moutakanni, Huy Vo, Marc Szafraniec, Vasil Khalidov, Pierre Fernandez, Daniel Haziza, Francisco Massa, Alaaeldin El-Nouby, et al. DINOv2: Learning Robust Visual Features without Supervision. *TMLR*, pages 1–31, 2024. 2, 3, 4, 6, 7
- [49] Vicente Ordonez, Girish Kulkarni, and Tamara Berg. Im2Text: Describing Images Using 1 Million Captioned Photographs. In *NeurIPS*, 2011. 4, 7

- [50] Long Ouyang, Jeffrey Wu, Xu Jiang, Diogo Almeida, Carroll Wainwright, Pamela Mishkin, Chong Zhang, Sandhini Agarwal, Katarina Slama, Alex Ray, et al. Training Language Models to Follow Instructions with Human Feedback. In *NeurIPS*, 2022. 2
- [51] Alec Radford, Jong Wook Kim, Chris Hallacy, Aditya Ramesh, Gabriel Goh, Sandhini Agarwal, Girish Sastry, Amanda Askell, Pamela Mishkin, Jack Clark, et al. Learning transferable visual models from natural language supervision. In *ICML*, 2021. 2, 3, 4, 6, 7
- [52] Colin Raffel, Noam Shazeer, Adam Roberts, Katherine Lee, Sharan Narang, Michael Matena, Yanqi Zhou, Wei Li, and Peter J Liu. Exploring the Limits of Transfer Learning with a Unified Text-to-Text Transformer. *JMLR*, 21(1):5485–5551, 2020. 2
- [53] Hanoona Rasheed, Muhammad Maaz, Salman Khan, and Fahad S. Khan. LLaVA++: Extending Visual Capabilities with LLaMA-3 and Phi-3, 2024. 2, 5
- [54] Christoph Schuhmann, Romain Beaumont, Richard Vencu, Cade Gordon, Ross Wightman, Mehdi Cherti, Theo Coombes, Aarush Katta, and Clayton others Mullis. LAION-5B: An open large-scale dataset for training next generation image-text models. In *NeurIPS*, 2022. 2, 4, 7
- [55] Baifeng Shi, Ziyang Wu, Maolin Mao, Xin Wang, and Trevor Darrell. When Do We Not Need Larger Vision Models? In *ECCV*, 2024. 3, 4, 6, 7
- [56] Amanpreet Singh, Vivek Natarajan, Meet Shah, Yu Jiang, Xinlei Chen, Dhruv Batra, Devi Parikh, and Marcus Rohrbach. Towards VQA Models That Can Read. In *CVPR*, 2019. 4
- [57] Nisan Stiennon, Long Ouyang, Jeffrey Wu, Daniel Ziegler, Ryan Lowe, Chelsea Voss, Alec Radford, Dario Amodei, and Paul F Christiano. Learning to Summarize with Human Feedback. In *NeurIPS*, 2020. 2
- [58] Rohan Taori, Ishaan Gulrajani, Tianyi Zhang, Yann Dubois, Xuechen Li, Carlos Guestrin, Percy Liang, and Tatsunori B Hashimoto. Stanford Alpaca: An Instruction-Following LLaMA Model, 2023. 2
- [59] Gemini Team, Rohan Anil, Sebastian Borgeaud, Jean-Baptiste Alayrac, Jiahui Yu, Radu Soricut, Johan Schalkwyk, Andrew M Dai, Anja Hauth, Katie Millican, et al. Gemini: A Family of Highly Capable Multimodal Models. *arXiv preprint arXiv:2312.11805*, 2023. 2
- [60] Gemma Team, Thomas Mesnard, Cassidy Hardin, Robert Dadashi, Surya Bhupatiraju, Shreya Pathak, Laurent Sifre, Morgane Rivière, Mihir Sanjay Kale, Juliette Love, et al. Gemma: Open Models Based on Gemini Research and Technology. *arXiv preprint arXiv:2403.08295*, 2024. 2
- [61] Gemma Team, Morgane Riviere, Shreya Pathak, Pier Giuseppe Sessa, Cassidy Hardin, Surya Bhupatiraju, Léonard Hussenot, Thomas Mesnard, Bobak Shahriari, Alexandre Ramé, et al. Gemma 2: Improving Open Language Models at a Practical Size. *arXiv preprint arXiv:2408.00118*, 2024. 1, 2, 3, 5
- [62] Peter Tong, Ellis Brown, Penghao Wu, Sanghyun Woo, Adithya Jairam Vedagiri IYER, Sai Charitha Akula, Shusheng Yang, Jihan Yang, Manoj Middepogu, Ziteng Wang, et al. Cambrian-1: A Fully Open, Vision-Centric Exploration of Multimodal LLMs. In *NeurIPS*, 2024. 3
- [63] Shengbang Tong, Zhuang Liu, Yuexiang Zhai, Yi Ma, Yann LeCun, and Saining Xie. Eyes Wide Shut? Exploring the Visual Shortcomings of Multimodal LLMs. In *CVPR*, 2024. 3
- [64] Hugo Touvron, Thibaut Lavril, Gautier Izacard, Xavier Martinet, Marie-Anne Lachaux, Timothée Lacroix, Baptiste Rozière, Naman Goyal, Eric Hambro, Faisal Azhar, et al. LLaMA: Open and Efficient Foundation Language Models. *arXiv preprint arXiv:2302.13971*, 2023. 1, 2
- [65] Hugo Touvron, Louis Martin, Kevin Stone, Peter Albert, Amjad Almahairi, Yasmine Babaei, Nikolay Bashlykov, Soumya Batra, Prajjwal Bhargava, Shriti Bhosale, et al. Llama 2: Open Foundation and Fine-Tuned Chat Models. *arXiv preprint arXiv:2307.09288*, 2023. 2
- [66] Michael Tschannen, Alexey Gritsenko, Xiao Wang, Muhammad Ferjad Naeem, Ibrahim Alabdulmohsin, Nikhil Parthasarathy, Talfan Evans, Lucas Beyer, Ye Xia, Basil Mustafa, et al. SigLIP 2: Multilingual Vision-Language Encoders with Improved Semantic Understanding, Localization, and Dense Features. *arXiv preprint arXiv:2502.14786*, 2025. 2, 3, 4, 6, 7
- [67] Hongyu Wang, Shuming Ma, Shaohan Huang, Li Dong, Wenhui Wang, Zhiliang Peng, Yu Wu, Payal Bajaj, Saksham Singhal, Alon Benhaim, et al. Magneto: A Foundation Transformer. In *ICML*, 2023. 2
- [68] Mitchell Wortsman, Gabriel Ilharco, Jong Wook Kim, Mike Li, Simon Kornblith, Rebecca Roelofs, Raphael Gontijo Lopes, Hannaneh Hajishirzi, Ali Farhadi, Hongseok Namkoong, and Ludwig Schmidt. Robust Fine-Tuning of Zero-Shot Models. In *CVPR*, 2022. 3
- [69] Linting Xue, Noah Constant, Adam Roberts, Mihir Kale, Rami Al-Rfou, Aditya Siddhant, Aditya Barua, and Colin Raffel. mT5: A massively multilingual pre-trained text-to-text transformer. *arXiv preprint arXiv:2010.11934*, 2020. 2
- [70] Xiang Yue, Yuansheng Ni, Kai Zhang, Tianyu Zheng, Ruoqi Liu, Ge Zhang, Samuel Stevens, Dongfu Jiang, Weiming Ren, Yuxuan Sun, et al. MMMU: A Massive Multi-discipline Multimodal Understanding and Reasoning Benchmark for Expert AGI. In *CVPR*, 2024. 5
- [71] Xiaohua Zhai, Basil Mustafa, Alexander Kolesnikov, and Lucas Beyer. Sigmoid Loss for Language Image Pre-Training. In *ICCV*, 2023. 2, 3, 4, 6, 7
- [72] Susan Zhang, Stephen Roller, Naman Goyal, Mikel Artetxe, Moya Chen, Shuohui Chen, Christopher Dewan, Mona Diab, Xian Li, Xi Victoria Lin, et al. OPT: Open Pre-trained Transformer Language Models. *arXiv preprint arXiv:2205.01068*, 2022. 2
- [73] Yichen Zhu, Minjie Zhu, Ning Liu, Zhiyuan Xu, and Yaxin Peng. LLaVA-Phi: Efficient Multi-Modal Assistant with Small Language Model. In *ACM Multimedia Workshops*, 2024. 5